

THE VERY RED AFTERGLOW OF GRB 000418: FURTHER EVIDENCE FOR DUST EXTINCTION IN A GAMMA-RAY BURST HOST GALAXY¹

S. KLOSE,² B. STECKLUM,² N. MASETTI,³ E. PIAN,³ E. PALAZZI,³ A. A. HENDEN,⁴ D. H. HARTMANN,⁵ O. FISCHER,⁶
J. GOROSABEL,⁷ C. SÁNCHEZ-FERNÁNDEZ,⁸ D. BUTLER,⁹ TH. OTT,⁹ S. HIPPLER,¹⁰ M. KASPER,¹⁰ R. WEISS,¹⁰
A. CASTRO-TIRADO,^{8,11} J. GREINER,¹² C. BARTOLINI,¹³ A. GUARNIERI,¹³ A. PICCIONI,¹³ S. BENETTI,¹⁴ F. GHINASSI,¹⁴
A. MAGAZZÚ,¹⁴ K. HURLEY,¹⁵ T. CLINE,¹⁶ J. TROMBKA,¹⁶ T. MCCLANAHAN,¹⁶ R. STARR,¹⁶ J. GOLDSTEN,¹⁷ R. GOLD,¹⁷
E. MAZETS,¹⁸ S. GOLENETSKII,¹⁸ K. NOESKE,¹⁹ P. PAPADEROS,¹⁹ P. M. VREESWIJK,²⁰ N. TANVIR,²¹ A. OSOZ,²²
J. A. MUÑOZ,²² AND J. M. CASTRO CERON²³

Received 2000 June 7; accepted 2000 August 3

ABSTRACT

We report near-infrared and optical follow-up observations of the afterglow of the GRB 000418 starting 2.5 days after the occurrence of the burst and extending over nearly 7 weeks. GRB 000418 represents the second case for which the afterglow was initially identified by observations in the near-infrared. During the first 10 days its *R*-band afterglow was well characterized by a single power-law decay with a slope of 0.86. However, at later times the temporal evolution of the afterglow flattens with respect to a simple power-law decay. Attributing this to an underlying host galaxy, we find its magnitude to be $R = 23.9$ and an intrinsic afterglow decay slope of 1.22. The afterglow was very red with $R - K \approx 4$ mag. The observations can be explained by an adiabatic, spherical fireball solution and a heavy reddening due to dust extinction in the host galaxy. This supports the picture that (long) bursts are associated with events in star-forming regions.

Subject heading: gamma rays: bursts

¹ Based on observations collected at the Bologna Astronomical Observatory in Loiano, Italy; at the TNG, Canary Islands, Spain; at the German-Spanish Astronomical Centre, Calar Alto, operated by the Max-Planck-Institut für Astronomie, Heidelberg, jointly with the Spanish National Commission for Astronomy; at the US Naval Observatory; and at the UK Infrared Telescope.

² Postal address: Thüringer Landessternwarte Tautenburg, D-07778 Tautenburg, Germany.

³ Istituto Tecnologie e Studio Radiazioni Extraterrestri, CNR, Via Gobetti 101, I-40129 Bologna, Italy.

⁴ US Naval Observatory, Flagstaff Station, P.O. Box 1149, Flagstaff, AZ 86002-1149.

⁵ Department of Physics and Astronomy, Clemson University, Clemson, SC 29634-1911.

⁶ Astrophysikalisches Institut und Universitäts-Sternwarte, Schiller-gässchen 2, D-07745 Jena, Germany.

⁷ Danish Space Research Institute, Juliane Maries Vej 30, DK-2100 Copenhagen, Denmark.

⁸ Laboratorio de Astrofísica Espacial y Física Fundamental (LAEFF-INTA), P.O. Box 50727, E-28080 Madrid, Spain.

⁹ Max-Planck-Institut für Extraterrestrische Physik, Giessenbachstrasse, D-85748 Garching, Germany.

¹⁰ Max-Planck-Institut für Astronomie, Königstuhl 17, D-69117 Heidelberg, Germany.

¹¹ Instituto de Astrofísica de Andalucía (IAA-CSIC), P.O. Box 03004, E-18080 Granada, Spain.

¹² Astrophysikalisches Institut Potsdam, D-14482 Potsdam, Germany.

¹³ Dipartimento di Astronomia, Università di Bologna, Via Ranzani 1, I-40127 Bologna, Italy.

¹⁴ Telescopio Nazionale Galileo, Centro Galileo Galilei, Calle Alvarez de Abreu 70, E-38700 Santa Cruz de La Palma, Canary Islands, Spain.

¹⁵ University of California at Berkeley, Space Sciences Laboratory, Berkeley, CA 94720-7450.

¹⁶ NASA Goddard Space Flight Center, Greenbelt, MD 20771.

¹⁷ Applied Physics Laboratory, Johns Hopkins University, Laurel, MD 20723.

¹⁸ Ioffe Physico-Technical Institute, St. Petersburg 194021, Russia.

¹⁹ Universitäts-Sternwarte, Geismarlandstrasse 11, D-37083 Göttingen, Germany.

²⁰ Astronomical Institute “Anton Pannekoehk,” Kruislaan 43, 1098 SJ Amsterdam, The Netherlands.

²¹ Joint Astronomy Centre, 660 North A’ohoku Place, Hilo, HI 96720.

²² Instituto de Astrofísica de Canarias, La Laguna, Tenerife, Spain.

²³ Real Observatorio de la Armada, San Fernando Naval, Cadiz, Spain.

1. INTRODUCTION

The detection of gamma-ray burst (GRB) afterglows still constitutes a challenge to observational astronomy. This is illustrated by the fact that three years after the discovery of GRB afterglows in the optical (van Paradijs et al. 1997) less than 20 such optical transients have been detected and followed up.²⁴ Among the afterglows recorded to date, the emission from GRB 000418 represents the second case for which the afterglow was initially identified in a gamma-ray burst error box by observations in the near-infrared (the first case is GRB 990705; Masetti et al. 2000).

GRB 000418 was observed on April 18.41 UT by the third interplanetary network (IPN), with *Ulysses* (Hurley et al. 1992) and the Near-Earth Asteroid Rendezvous mission (NEAR, XGRS detector; Goldsten et al. 1997) as its distant points and GGS-Wind Konus (Aptekar et al. 1995) close to Earth. The burst had a duration of ~ 30 s and a fluence in the 25–100 keV range of $\sim 1.3 \times 10^{-5}$ ergs cm^{-2} (Hurley, Cline, & Mazets 2000). These properties characterize the event as a long, relatively bright GRB (cf. Fishman & Meegan 1995).

Rapid follow-up and second-epoch near-infrared (NIR) observations of the central part of the 35 arcmin²-sized GRB error box led to the detection of an NIR source (Klose et al. 2000) at R.A. (J2000) = 12^h25^m19^s.30, decl. (J2000) = 20°06′11″.6 ($\pm 0″.5$), whose fading nature was quickly confirmed by follow-up observations in the optical (Mirabal, Halpern, & Wagner 2000c). The fading of the afterglow is clearly illustrated in Figure 1 which reports *R*-band images taken at Telescopio Nazionale Galileo on 2000 April 20 and June 2. The successful detection of the afterglow of GRB 000418 makes this an afterglow of an “IPN only” burst,

²⁴ See J. Greiner, 2000, <http://www.aip.de/~jcg/grbgen.html> for continuous updates.

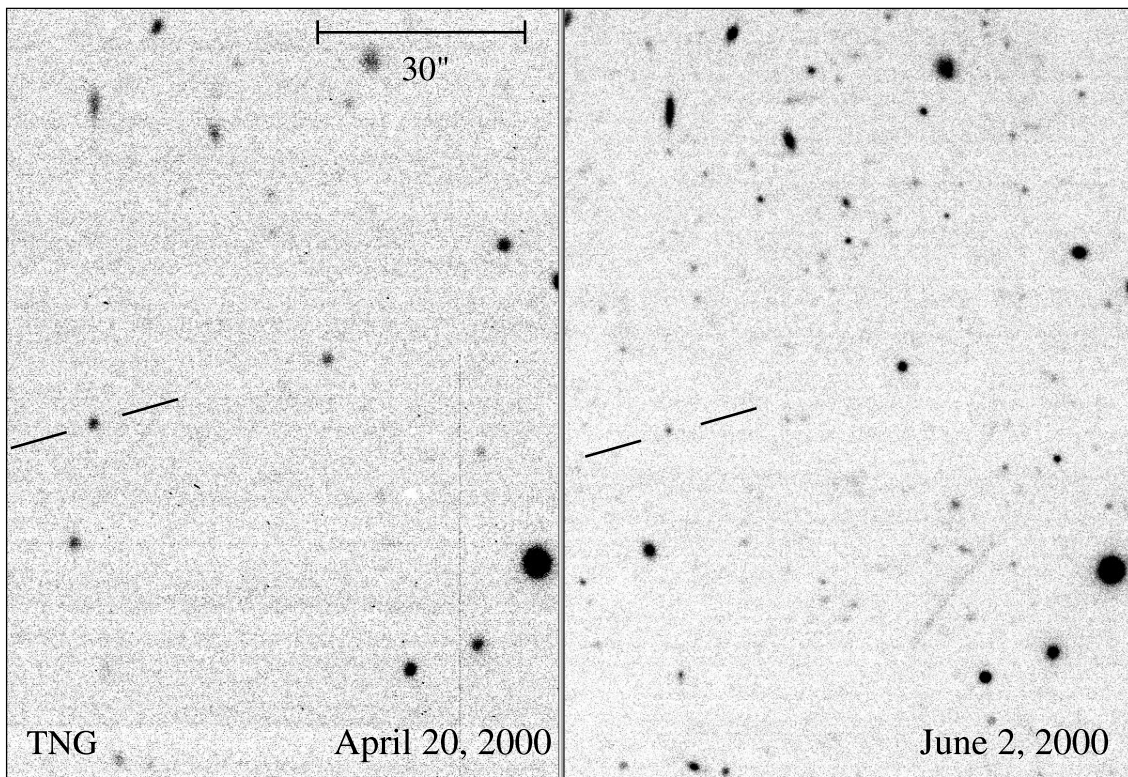


FIG. 1.—Finding chart for the field of GRB 000418. The afterglow is indicated. *Left panel*: R-band image taken with the TNG telescope on April 20.9 UT. *Right panel*: R-band image taken with TNG on June 2.9 UT (Table 1). North is up, east is left.

with no additional available X-ray (*BeppoSAX*) or BATSE spectral information (GRB 991208 was the first of these bursts with detected optical afterglow; Hurley et al. 2000; Castro-Tirado et al. 2000). Triggered by the NIR detection of the afterglow of GRB 000418, many observatories worldwide directed their attention to this burst. Here we report on a subset of these activities, with emphasis on the R-band light curve.

2. OBSERVATIONS AND DATA REDUCTION

The IPN error box of GRB 000418 became known two days after the burst. The observations leading to the discovery of the GRB afterglow were performed on 2000 April 20 and April 22 with the 3.5 m telescope on Calar Alto, Spain, equipped with the near-infrared camera Omega Cass (Lenzen et al. 1998) which was operated in the polarimetric mode. The central part of the elongated GRB error box was imaged with the 3.5 m telescope in the course of a target of opportunity project. In the polarimetric wide-field mode, the Omega Cass camera has a $5' \times 5'$ field of view and an image scale of $0''.3 \text{ pixel}^{-1}$. The limiting magnitude of the K' -band image is ~ 18.5 for unpolarized objects after adding all frames taken at different position angles of the wire-grid polarizer.

Further near-infrared observations were performed at the Calar Alto 1.23 m telescope using the NIR camera MAGIC, with the United Kingdom Infrared Telescope (UKIRT) equipped with the UKIRT Fast-Track Imager and using the Calar Alto 3.5 m telescope equipped with the Omega Prime near-infrared camera (Table 1). Optical follow-up observations were performed at the Italian Telescopio Nazionale Galileo (TNG), La Palma, Spain; at the US

Naval Observatory Flagstaff Station (NOFS); at the 1.52 m “G. D. Cassini” telescope of the University of Bologna in Loiano, Italy; and on Calar Alto using the 3.5 m telescope with the multipurpose instrument MOSCA. TNG is equipped with the Optical Imager Galileo camera, which contains two EEV CCDs. The Loiano telescope employs the Bologna Faint Object Spectrograph and Camera, equipped with an EEV CCD. The NOFS observations were performed with either the 1.3 m automated telescope, equipped with a SITe CCD, or the 1.0 m telescope, equipped with a Tektronix CCD.

The K' -band measurements performed on April 20.90 UT were reduced in a standard fashion. The sky contribution was obtained from the median of the dithered images and, in combination with a proper dark frame, used to derive the flat field. The images were sky subtracted, flat-fielded, bad pixel corrected, and finally mosaicked. This procedure was performed for each orientation of the polarimetric analyzer. The final image is the sum of the frames obtained for each orientation of the polarizer. Unfortunately, it was not possible to derive the linear polarization from these frames. The Calar Alto 3.5 m data of April 22 were obtained during variable sky and required another method to estimate the flat field. The considerable temporal variation of the sky background allowed the derivation of both the flat field and bias by pixelwise linear regression, similar to the scheme proposed by Fixsen, Moseley, & Arendt (2000). Otherwise, the image processing was the same.

We determined the K' -band magnitude of the afterglow by means of optical photometry of secondary standard stars in the field around the burster (Henden 2000) and by means of the USNO-SA2.0 Catalog (Monet et al. 1996). The basic

TABLE 1
SUMMARY OF OBSERVATIONS OF GRB 000418

Date	$t - t_0^a$	Telescope ^b	Exposure (s)	Filter	Magnitude	Reference
Apr 20.89 UT	2.48	TNG 3.5 m	600	R	21.63 ± 0.04	1
Apr 20.90 UT	2.49	Calar Alto 3.5 m	1200	K'	$17.5 \pm 0.50^{c,d}$	2
Apr 20.93 UT	2.52	Calar Alto 1.23 m	3600	K'	17.9 ± 0.20	1
Apr 20.94 UT	2.53	Loiano 1.52 m	3×1200	R	> 20.5	1
Apr 21.15 UT	2.74	MDM 2.4 m		R	21.77 ± 0.12^c	3
Apr 21.86 UT	3.45	Loiano 1.52 m	3×1200	R	22.01 ± 0.14	1
Apr 21.94 UT	3.53	Calar Alto 1.23 m	1350	J	> 18	1
Apr 22.12 UT	3.71	Calar Alto 3.5 m	1200	K'	$> 18.3^d$	1
Apr 24.92 UT	6.51	Calar Alto 1.23 m	4095	K'	> 17.5	1
Apr 26.32 UT	7.91	NOFS 1.3 m	3×600	R	22.74 ± 0.20^e	4
Apr 27.26 UT	8.85	MDM 2.4 m		R	22.84 ± 0.23^e	5
Apr 28.3 UT	9.89	MDM 2.4 m		R	23.05 ± 0.31^e	6
May 02.31 UT	13.90	NOFS 1.3 m	21×600	R	23.20 ± 0.13	1
May 03.26 UT	14.85	NOFS 1.3 m	36×600	R	23.50 ± 0.16	1
May 04.44 UT	16.03	UKIRT 3.8 m	3240	K	20.50 ± 0.4	1
May 06.42 UT	18.01	Keck I 10 m		R	23.57 ± 0.10	7
May 08.89 UT	20.48	TNG 3.5 m	3×600	R	23.39 ± 0.05	1
May 08.92 UT	20.51	TNG 3.5 m	3×600	V	24.03 ± 0.07	1
May 09.82 UT	21.41	NOFS 1.0 m	12×1200	R	23.46 ± 0.21	1
May 11.95 UT	23.54	Calar Alto 3.5 m	2100	J	> 19.5	1
May 15.01 UT	26.60	Calar Alto 3.5 m	840	J	> 20.5	1
May 15.02 UT	26.61	Calar Alto 3.5 m	1680	K'	> 19.5	1
May 23.93 UT	35.52	TNG 3.5 m	3×900	R	23.46 ± 0.10	1
Jun 02.88 UT	45.47	Calar Alto 3.5 m	4×600	R	23.41 ± 0.08	1
Jun 02.91 UT	45.50	TNG 3.5 m	3×1200	R	23.66 ± 0.05	1

NOTE.—Supplemented by data taken from the literature.

^a t_0 is the time of the occurrence of the burst: April 18.41 UT.

^b TNG: Telescopio Nazionale Galileo, La Palma, Spain; NOFS: US Naval Observatory Flagstaff Station; Loiano: G. D. Cassini telescope of the University of Bologna, Loiano, Italy; MDM: Hiltner telescope at the MDM Observatory on Kitt Peak; UKIRT: United Kingdom Infrared Telescope, Mauna Kea, Hawaii.

^c Affected by a bad focus.

^d Reduced sensitivity due to polarimetric mode.

^e Corrected according to improved photometry of secondary standard stars by Henden 2000.

REFERENCES.—(1) This paper; (2) Stecklum et al. 2000; (3) Mirabal et al. 2000a; (4) Henden et al. 2000; (5) Mirabal et al. 2000b; (6) Mirabal et al. 2000c; (7) Metzger & Fruchter 2000.

assumptions in our procedure are that the selected field stars are main-sequence stars and that their optical colors are representative for their spectral type. We corrected our

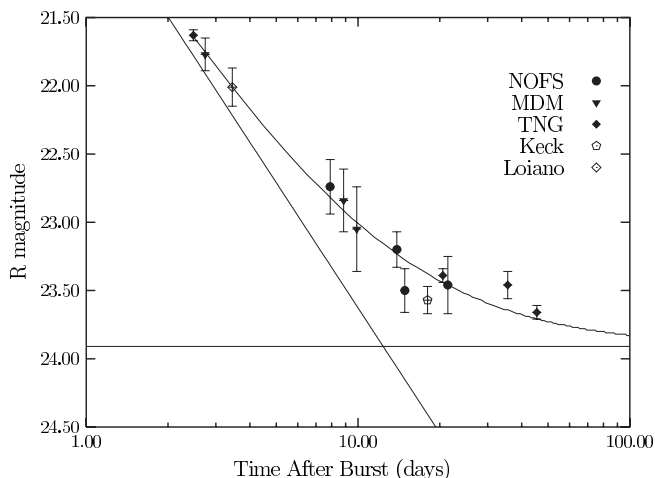


FIG. 2.—R-band light curve of GRB 000418. The solid line is the best fit to the data which predicts an underlying host galaxy with $R = 23.9$. The straight lines show the individual contributions of the GRB afterglow (following a power-law decay with $\alpha = 1.22$) and the host galaxy to the total observed flux.

K' -band data for differences in the K , K' magnitudes using the relation $K' - K = 0.20(H - K)$ (Wainscoat & Cowie 1992). The $H - K$ color of the afterglow was calculated based on the $R - K'$ color measured on April 20.9 UT (Table 1) and assuming an $F_\nu \propto \nu^{-\beta}$ optical-NIR spectrum (see below); this gives $K' - K \approx 0.2$ mag. Finally, we used the wide-field K' -band image obtained at Calar Alto on May 15 to calibrate the narrow-field UKIRT K -band image from May 4. Although the photometry of our NIR data is not as accurate as our R -band photometry, this does not affect the basic content of the following discussion (§ 3). The R -band light curve is shown in Figure 2.

Because GRB 000418 was at high Galactic latitude, we assume that the faint photometric reference stars exhibit the same Galactic extinction as the GRB afterglow. The Schlegel, Finkbeiner, & Davis (1998) extinction maps predict $E(B - V) = 0.04$ through the Galaxy along Galactic coordinates $(l, b) = 265^\circ.1, 80^\circ.5$. Assuming a ratio of visual to selective extinction of 3.1, this gives $A_V \sim 0.12$ mag. The dust distribution model of Chi & Wolfendale (1991) predicts a larger visual extinction of $A_V \sim 0.19$ mag, while the compilation of Hakkila et al. (1997) predicts a very small value of $A_V \sim 0.02$ mag. We take the value derived from Schlegel et al., which is close to the mean of the latter two estimates. Then, according to Rieke & Lebofsky (1985), this corresponds to $A_R = 0.09$ mag and $A_K = 0.01$ mag.

For the R -band optical frames, point-spread function fitting was performed using DAOPHOT-II as implemented in IRAF. The deep frames provided a means to find isolated, well-sampled stars in a field highly contaminated by galaxies. These stars were used to calculate mean point-spread functions, and the instrumental magnitudes of the optical transient and several comparison stars were extracted. The comparison star standard R -band magnitudes were obtained from the field photometry file of Henden (2000) and the afterglow magnitude determined differentially with respect to the ensemble mean.

3. RESULTS AND DISCUSSION

GRB 000418 is an “IPN only” burst, and its afterglow was not observed in the X-ray band. Moreover, radio observations of GRB 000418 were not performed before April 29 (Frail 2000). The lack of these data limits the diagnostic power of afterglow observations in this case, but the optical decay still yields a significant parameter (the slope of the decay law), and future changes in slope might yet provide evidence for beaming or contamination by light from an underlying supernova. Therefore, we concentrate here on the interpretation of the optical/NIR afterglow of this burst. We follow the “standard procedure” (e.g., Wijers, Rees, & Mészáros 1997; Galama et al. 1998; Frail, Waxman, & Kulkarni 2000) for interpreting afterglows within the context of the so-called fireball model. In this widely accepted model for GRB afterglows, the spectral signature is due predominantly to synchrotron emission from relativistic electrons accelerated in the strong shock wave that propagates into the burst environment (and also a reverse shock propagating into the burst ejecta, in close analogy to the situation in supernova remnants, with the exception that GRBs produce highly relativistic shocks). The emerging spectrum is a combination of emission from internal shocks (energy dissipation within the ejecta) and external shocks driven into a medium that could be roughly uniform (ISM-like) or have strong radial profiles, as would be the case if the external medium is wind material from a massive star prior to becoming a collapsar. The basic properties of these relativistic shock models are reviewed by Piran (1999) and Mészáros (2000). In the simplest model (an impulsive blast wave, a uniform circumburst medium, and spherical symmetry), the evolution of the afterglow flux density evolves according to a power law in time, i.e., $F_\nu(t) \sim t^{-\alpha} \nu^{-\beta}$ once the synchrotron peak has moved through the bandpass. The time-dependent apparent magnitude in a given photometric band is then described by $m(t_2) - m(t_1) = 2.5\alpha \lg(t_1/t_2)$, where t is measured from the time of the occurrence of the burst (see Vrba et al. 2000 for a discussion of the zero point of t). Possible deviations from a power-law decay of the afterglow flux can be caused by a variety of reasons (see Rhoads & Fruchter 2000 for a recent discussion): different afterglow physics and model assumptions about the environment (cf. Panaitescu, Mészáros, & Rees 1998), a jet geometry (cf. Sari, Piran, & Halpern 1999), supernova light which adds to the afterglow flux (cf. Bloom et al. 1999), light echoes due to dust clouds around the burst (e.g., Esin & Blandford 2000), or an emerging host galaxy which becomes detectable when the afterglow is faint enough (cf. Zharikov, Sokolov, & Baryshev 1998). Most afterglows are very faint in the optical, even at early times, and therefore are usually observed at the detection limit of optical telescopes. An observational search for deviations

from the prediction of the simplest fireball model is therefore difficult in most cases. GRB 000418 is no exception to this.

If we consider only the first five data points of the afterglow light curve (Fig. 2), then the best-fit temporal power-law slope is $\alpha = 0.86 \pm 0.06$ ($\chi^2/\text{dof} = 0.31$), in agreement with Mirabal, Halpern, & Wagner (2000b) and Mirabal et al. (2000c). However, starting in May (after 10 days since the GRB trigger) the R -band data indicate a significant flattening with respect to the predicted power-law decay of the afterglow flux with $\alpha = 0.86$. Light from an underlying host galaxy can explain this discrepancy. The best fit now is $\alpha = 1.22$ and $R_{\text{host}} = 23.9$ ($\chi^2/\text{dof} = 2.18$). (In this fit we have omitted the single Calar Alto R -band data point from June 2. If we include it we get $\alpha = 1.29$, $R_{\text{host}} = 23.8$.)

At the time of the K' -band observation (April 20.9 UT), the afterglow was very red with $R-K = 3.9 \pm 0.2$ mag (Table 1). A similar red color was observed for GRB 980329 (Palazzi et al. 1998) and GRB 990705 (Masetti et al. 2000). If we take reddening by Galactic dust into account (§ 2), then, on April 20.9 UT, the observed spectral slope across the $R-K$ band is $\beta = 1.90 \pm 0.15$, where the uncertainty is dominated by the error of the K' -band magnitude. The slow power-law decay of the afterglow, $\alpha = 1.22$, favors spherically symmetric evolution (Table 2). Following the analysis of Sari, Piran, & Narayan (1998) for a shock expanding into a uniform medium, the predicted value for the spectral slope β across the $R-K$ passband is $(2\alpha - 1)/3 = 0.48$ or $2\alpha/3 = 0.81$, respectively, depending on whether or not the bulk of the radiating electrons is in the fast-cooling regime, i.e., whether or not the characteristic cooling time is shorter than the age of the shock. Since our observations started several hours after the GRB, we expect that at this time the bulk of the electrons was already in the slow-cooling regime. The slope p of the power-law distribution of electron Lorentz factors, $N(\gamma)d\gamma \sim \gamma^{-p}d\gamma$, is then $p = 4\alpha/3 + 1 = 2.63$. The fact that the observed spectral index β significantly exceeds the predicted value could plausibly be a consequence of extinction in the host galaxy.

Extinction in the host galaxy may change the spectral energy distribution (SED) of the afterglow in the optical/NIR bands such that the SED in the optical/NIR range can no longer be approximated by a single power law. This renders the color estimate redshift dependent. Assuming that the local extinction in the GRB environment is dominated by dust, we corrected the observed optical/NIR spectral slope of the afterglow by adopting a local optical extinction curve $A(\lambda)$ in the GRB environment which is similar to that for the Galactic interstellar dust (Sudžiūsis, Bobinas, & Raudeliūnas 1996). However, we let the ratio of total to selective extinction, R_{dust} , be a free parameter, in order to describe approximately the various extinction curves found in star-forming regions in our Galaxy (e.g., Vrba, Coyne, & Tapia 1993) and in starburst galaxies (e.g., Calzetti 1997). For a redshift of $z = 1.118$ (Bloom et al. 2000) and a Galactic visual extinction in the direction of the optical transient of $A_V = 0.12$ mag (§ 2), we find that a visual extinction in the host galaxy of $A_V^{\text{host}} \sim (0.96 \pm 0.2)R_{\text{dust}}/3.17$ mag is required in order to change the spectral index from $\beta = 0.81$ to the observed one, assuming no contribution from the underlying host galaxy. We thus conclude that the observed optical/NIR color can in principle be forced to agree with the observed power-law decline slope *if*, on April 20.9 UT, the observations were carried out

TABLE 2
R-BAND GRB AFTERGLOWS WITH WELL-OBSERVED POWER-LAW BREAKS

GRB	Redshift	Reference	α_1	t_{break} (days)	α_2	Reference
990123	1.600	1	1.13 ± 0.02	1.75 ± 0.25	1.75 ± 0.11	2
	1.600	3	1.10 ± 0.03	2.04 ± 0.46	1.65 ± 0.06	4
990510	1.619	5	0.82 ± 0.02	1.20 ± 0.08	2.18 ± 0.05	6
			0.75 ± 0.03	1.30 ± 0.10	2.46 ± 0.06	7
			0.82 ± 0.03	1.51 ± 0.09	2.23 ± 0.07	8
			0.76 ± 0.01	1.75 ± 0.03	2.40 ± 0.02	9
000301c	2.03	10	0.92	6.30	3.11	11
			0.72 ± 0.34	4.39 ± 1.52	2.29 ± 1.00	12

NOTE.— α_1 describes the early power-law decay, α_2 the late-time power-law decay; t_{break} is the break time.

REFERENCES.—(1) Andersen et al. 1999; (2) Castro-Tirado et al. 1999a; (3) Kelson et al. 1999, Hjorth et al. 1999; (4) Kulkarni et al. 1999; (5) Vreeswijk et al. 1999b; (6) Harrison et al. 1999; (7) Israel et al. 1999; (8) Beuermann et al. 1999; (9) Stanek et al. 1999; (10) Castro et al. 2000; (11) Rhoads & Fruchter 2000; (12) Jensen et al. 2000.

at a time when the effects of jet formation were not manifest, i.e., the light curve is well represented by the adiabatic, spherical fireball solution (e.g., Wijers et al. 1997; Sari et al. 1998), and the afterglow was significantly reddened due to dust extinction in the host galaxy. While this argument supports the notion that the GRB was associated with a massive star embedded in a star-forming region (e.g., Paczyński 1998; Fryer, Woosley, & Hartmann 1999), the optical/NIR observations alone cannot constrain the position of the intervening dust in the GRB host galaxy. We note, however, that our value for A_V^{host} is comparable to those deduced from observations of the optical afterglows of GRB 980703 (Castro-Tirado et al. 1999b; Vreeswijk et al. 1999a), GRB 971214 (Dal Fiume et al. 2000; Halpern et al. 1998; Ramaprakash et al. 1998), and GRB 980329 (Palazzi et al. 1998).

Combining the May 3.3 UT *R*-band measurement with the May 4.4 UT *K*-band data gives a color of the afterglow of $R - K = 3.0 \pm 0.4$ mag. Within our measurement errors this is not in conflict with our April 20.9 data, assuming that the color is now affected by the color of the underlying host galaxy. On May 8.9 UT (day 20.5), we measure $V - R = 0.64$ which also indicates that the optical spectrum is less steep at later times. The $R - K$ color value for the afterglow, together with the assumption of a flat spectrum for the host, suggests that on May 8.9 the main contribution to the measured *V* magnitude is due to the host galaxy, as we derive $V_{\text{host}} \sim 24.2$ (and $K_{\text{host}} \sim 22.1$) in this hypothesis. Our imaging, however, does not reveal the GRB host galaxy as an extended structure. The source remains point-like. We have compared the TNG image from April 20 with the TNG image obtained on May 23 in order to get an information about the displacement d of the GRB afterglow from the luminosity center of the host galaxy. In the TNG image from April 20 the point-spread function (PSF) of the source is mainly determined by the GRB afterglow, whereas in the TNG image from May 23 it is mainly determined by the host galaxy. This allowed us to check if there is evidence for a shift of the center of the PSF with respect to a nearby reference star. We found no evidence for such a shift and conclude $d < 0''.1$.

Initially, the observed temporal power-law decay of the afterglow of GRB 000418 was somewhat similar to that observed in the early light curve of GRB 990510 (Table 2); the timescale, however, was notably different. The afterglow

of GRB 990510 was slow for only about the first 24 hr, afterwards steepening to $\alpha > 2$. By contrast, the afterglow of GRB 000418 displayed this slow decay mode for the first 10 days (see Vrba et al. 2000 for a compilation of other late-time temporal power-law slopes). With the underlying host galaxy becoming apparent in the afterglow flux, the deduced temporal slope $\alpha = 1.22$ brings this burst now close to GRBs 970228, 970508 (Garcia et al. 1998), and 971214 (Kulkarni et al. 1998; Ramaprakash et al. 1998).

4. CONCLUSIONS

Based on the *R*-band data alone, the parameters characterizing a GRB afterglow are not strongly constrained. In general, the two observational parameters easiest to determine in the optical with reasonable accuracy are the temporal power-law decay slope, α , and the redshift of the GRB host, if present. The spectral slope, β , is affected by extinction and thus much less accurately known, and model dependent. On the other hand, even the deduced parameter α can be misleading if the observed temporal evolution of the afterglow flux is affected by an underlying host galaxy which becomes visible only at later times (cf. Castro-Tirado & Gorosabel 1999). The database available to us is not sufficient to distinguish between the various nonstandard afterglow models, like a blast into a uniform medium versus a shock expanding into a preexisting stellar wind with a circumburst density profile $\rho \propto r^{-2}$, or the possible effects from anisotropic outflows (Mészáros, Rees, & Wijers 1998; Chevalier & Li 1999). In particular, the GRB afterglow decline slope α is not very steep, which hampers an unambiguous detection of a supernova component in the afterglow (cf. Bloom et al. 1999). The observational evidence which we found for a reddening of the afterglow in the GRB host galaxy supports, however, the picture that the GRB was associated with a dusty star-forming region.

The redshift of GRB 000418 has been estimated from a line doublet attributed to [O II] emitted by the host galaxy (Bloom et al. 2000). With this preliminary identification the redshift is $z = 1.118$, which is close to the mean of the current redshift database. Assuming spherical emission, the energy release in gamma rays of GRB 000418 was thus about 5×10^{52} ergs (Bloom et al. 2000), and the total observed fluence in the *R*-band between day 2.5 and day 50 is about 0.03% of the energy in the gamma-ray regime. The energy release in gamma rays is about 2 orders of magni-

tude less luminous than the current record for GRB 990123 (Andersen et al. 1999; Kulkarni et al. 1999). It places this burst near the median of the dozen presently determined energy releases (see Klose 2000 for a recent review). If the brightest bursts are those with the smallest collimation angles (in order to reduce the energy requirements), GRB 000418 might not be strongly beamed. Indeed, based on our data, covering day 2 to day 50 after the burst, we do not find evidence for a noticeable break in the light curve, which would be the telltale signature of an emerging view of the jet's edge. Moreover, within the context of the fireball model (e.g., Wijers et al. 1997; Sari et al. 1998), we can explain the optical/NIR data with the simple spherical solution. Since the observations of this afterglow do not cover the first 2 days, we are unable to state with certainty that we have not missed any break in the early light curve. However, if that had been the case the early power-law decay would have been even slower, i.e., $\alpha < 1$, which would make it close to that of GRB 970508 (e.g., Castro-Tirado et al. 1998) and perhaps place the spectrum in the $F_\nu \sim \nu^{1/3}$ regime with $-\frac{1}{2} < \alpha < \frac{1}{3}$ (Sari et al. 1998).

GRB 000418 is only the ~ 10 th burst for which a well-observed afterglow light curve has been established. This

case continues to support the basic concepts of the fireball scenario, but it also reminds us that every afterglow is unique and that a large database will be required to establish the dynamic range of afterglow properties.

Note added in manuscript.—When this paper was submitted Bloom et al. (2000, GCN Circ. 689) and Metzger et al. (2000, GCN Circ. 733) reported the detection of the GRB host galaxy at $R = 24 \pm 0.3$ and $R = 23.9 \pm 0.2$, respectively, in agreement with our fit to the light curve.

S. K. acknowledges valuable comments by Fred Vrba, Flagstaff, and Attila Mészáros, Prague. J. Gorosabel acknowledges the receipt of a Marie Curie Research Grant from the European Commission. This work has been partially supported by the Spanish INTA grant Rafael Calvo Rodés and the Spanish CICYT grant ESP95-0389-C02-02. K. H. is grateful for *Ulysses* support under JPL contract 958056 and for NEAR support under NAG 5-9503. We thank the staff of the Calar Alto observatory for performing service observations. We thank the referee, D. Helfand, for his constructive remarks.

REFERENCES

- Andersen, M. I., et al. 1999, *Science*, 283, 2075
 Aptekar, R., et al. 1995, *Space Sci. Rev.*, 71, 265
 Beuermann, K., et al. 1999, *A&A*, 352, L26
 Bloom, J. S., et al. 1999, *Nature*, 401, 453
 Bloom, J. S., et al. 2000, GCN Circ. 661 (<http://gcn.gsfc.nasa.gov/gcn/gcn3/661.gcn3>)
 Calzetti, D. 1997, *AJ*, 113, 162
 Castro, S. M., et al. 2000, GCN Circ. 605 (<http://gcn.gsfc.nasa.gov/gcn/gcn3/605.gcn3>)
 Castro-Tirado, A. J., et al. 1998, *Science*, 279, 1011
 ———, 1999a, *Science*, 283, 2069
 ———, 1999b, *ApJ*, 511, L85
 ———, 2000, *A&A*, submitted
 Castro-Tirado, A. J., & Gorosabel, J. 1999, *A&AS*, 138, 449
 Chevalier, R. A., & Li, Z.-Y. 1999, *ApJ*, 520, L29
 Chi, X., & Wolfendale, A. W. 1991, *J. Phys. G*, 17, 987
 Dal Fiume, D., et al. 2000, *A&A*, 355, 454
 Esin, A. A., & Blandford, R. 2000, *ApJ*, 534, L151
 Fishman, G. J., & Meegan, C. A. 1995, *ARA&A*, 33, 415
 Fixsen, D. J., Moseley, S. H., & Arendt, R. G. 2000, *ApJS*, 128, 651
 Frail, D. A. 2000, GCN Circ. 655 (<http://gcn.gsfc.nasa.gov/gcn/gcn3/655.gcn3>)
 Frail, D. A., Waxman, E., & Kulkarni, S. R. 2000, *ApJ*, 537, 191
 Fryer, C. L., Woosley, S. E., & Hartmann, D. H. 1999, *ApJ*, 526, 152
 Galama, T. J., et al. 1998, *ApJ*, 500, L97
 Garcia, M. R., et al. 1998, *ApJ*, 500, L105
 Goldsten, J., et al. 1997, *Space Sci. Rev.*, 82, 169
 Hakkila, J., Myers, J., Stidham, B., & Hartmann, D. H. 1997, *AJ*, 114, 2043
 Halpern, J. P., Thorstensen, J. R., Helfand, D. J., & Costa, E. 1998, *Nature*, 393, 41
 Harrison, F. A., et al. 1999, *ApJ*, 523, L121
 Henden, A. A. 2000, GCN Circ. 662 (<http://gcn.gsfc.nasa.gov/gcn/gcn3/662.gcn3>)
 Henden, A. A., et al. 2000, GCN Circ. 652 (<http://gcn.gsfc.nasa.gov/gcn/gcn3/652.gcn3>)
 Hjorth, J., et al. 1999, GCN Circ. 219 (<http://gcn.gsfc.nasa.gov/gcn/gcn3/219.gcn3>)
 Hurley, K., Cline, T., & Mazets, E. 2000, GCN Circ. 642 (<http://gcn.gsfc.nasa.gov/gcn/gcn3/642.gcn3>)
 Hurley, K., et al. 1992, *A&AS*, 92, 401
 ———, 2000, *ApJ*, 534, L23
 Israel, G. L., et al. 1999, *A&A*, 348, L5
 Jensen, B. L., et al. 2000, *A&A*, submitted (astro-ph/0005609)
 Kelson, D. D., et al. 1999, *IAU Circ.* 7096
 Klose, S. 2000 in *Reviews in Modern Astronomy* 13, ed. R. E. Schielicke (Hamburg: Astronomische Gesellschaft), 129
 Klose, S., et al. 2000, GCN Circ. 645 (<http://gcn.gsfc.nasa.gov/gcn/gcn3/645.gcn3>)
 Kulkarni, S. R., et al. 1998, *Nature*, 393, 35
 ———, 1999, *Nature*, 398, 389
 Lenzen, R., Bizenberger, P., Salm, N., & Storz, C. 1998, *Proc. SPIE*, 3354, 493
 Masetti, N., et al. 2000, *A&A*, 354, 473
 Mészáros, P. 2000, *Nucl. Phys. B*, 80, 63
 Mészáros, P., Rees, M. J., & Wijers, R. A. M. J. 1998, *ApJ*, 499, 301
 Metzger, M. R., & Fruchter, A. 2000, GCN Circ. 669 (<http://gcn.gsfc.nasa.gov/gcn/gcn3/669.gcn3>)
 Mirabal, N., Halpern, J. P., Kemp, J., & Helfand, D. J. 2000a, GCN Circ. 646 (<http://gcn.gsfc.nasa.gov/gcn/gcn3/646.gcn3>)
 Mirabal, N., Halpern, J. P., & Wagner, R. M. 2000b, GCN Circ. 650 (<http://gcn.gsfc.nasa.gov/gcn/gcn3/650.gcn3>)
 ———, 2000c, GCN Circ. 653 (<http://gcn.gsfc.nasa.gov/gcn/gcn3/653.gcn3>)
 Monet, D., et al. 1996, USNO-SA2.0 (Washington, DC: US Naval Observatory)
 Paczyński, B. 1998, *ApJ*, 494, L45
 Palazzi, E., et al. 1998, *A&A*, 336, L95
 Panaitescu, A., Mészáros, P., & Rees, M. J. 1998, *ApJ*, 503, 314
 Piran, T. 1999, *Phys. Rep.*, 314, 575
 Ramaprakash, A. N., et al. 1998, *Nature*, 393, 43
 Rhoads, J. E., & Fruchter, A. S. 2000, *ApJ*, in press
 Rieke, G. H., & Lebofsky, M. J. 1985, *ApJ*, 288, 618
 Sari, R., Piran, T., & Halpern, R. 1999, *ApJ*, 519, L17
 Sari, R., Piran, T., & Narayan, R. 1998, *ApJ*, 497, L17
 Schlegel, D., Finkbeiner, D., & Davis, M. 1998, *ApJ*, 500, 525
 Stanek, K. Z., et al. 1999, *ApJ*, 522, L39
 Stecklum, B., et al. 2000, GCN Circ. 654 (<http://gcn.gsfc.nasa.gov/gcn/gcn3/654.gcn3>)
 Sūdzius, J., Bobinas, V., & Raudeliūnas, S. 1996, *Baltic Astron.*, 5, 485
 van Paradijs, J., et al. 1997, *Nature*, 386, 686
 Vrba, F. J., Coyne, G. V., & Tapia, S. 1993, *AJ*, 105, 1010
 Vrba, F. J., et al. 2000, *ApJ*, 528, 254
 Vreeswijk, P. M., et al. 1999a, *ApJ*, 523, 171
 ———, 1999b, GCN Circ. 324 (<http://gcn.gsfc.nasa.gov/gcn/gcn3/324.gcn3>)
 Wainscoat, R. J., & Cowie, L. L. 1992, *AJ*, 103, 332
 Wijers, R. A. M. J., Rees, M. J., & Mészáros, P. 1997, *MNRAS*, 288, L51
 Zharikov, S. V., Sokolov, V. V., & Baryshev, Yu. V. 1998, *A&A*, 337, 356